Malaysian Journal of Chemistry, 2025, Vol. 27(2), 197-216

Enzymatic and Microbial-Assisted Treatments for the Extraction of Agarwood Essential Oils and Authentication using FTIR-ATR Spectroscopy and Multivariate Data Analysis

Muhammad Zulhelmi Nazri[1], Norliza Abdul Latiff[1], Siti Nor Azlina Abd Rashid[1], Salimah Ab Malik[1], Ariffi Suraya Rahmani[1], Nooraina Atira Alaudin[1], Nur Fashya Musa[1], Zaheda Mohamad Azam[1], Khairunnisa Embi[1] and Norazah Basar[1,2]*

[1]Innovation Centre in Agritechnology for Advanced Bioprocessing (ICA), Universiti Teknologi Malaysia (UTM), Pagoh, Johor, Malaysia

[2]Department of Chemistry, Faculty of Science, Universiti Teknologi Malaysia (UTM), Skudai, Johor Bahru, Johor, Malaysia

*Corresponding author (e-mail: norazahb@utm.my)

Agarwood essential oil is a highly prized natural product known for its unique fragrance and therapeutic properties. This study explores the use of enzymatic and microbial-assisted treatments for enhanced extraction of agarwood essential oils, aiming to improve the yield and quality while maintaining sustainability. Moreover, advanced Fourier transform infrared spectroscopy with attenuated total reflectance (FTIR-ATR) was employed for rapid characterization through functional and fingerprint regions comprising of the wavenumber region of 4000 – 400 cm^{-1} of the essential oils. The multivariate data analysis techniques, including discriminant (DA), partial least squares-discriminant (PLS-DA) and principal component (PCA) analyses, were applied to the FTIR-ATR spectra as to differentiate the essential oil samples based on their chemical profiles of different essential oil extractions. The findings reveal that enzymatic and microbial treatments significantly enhance the efficiency of essential oil extraction, yielding sufficient volumes of essential oils. The FTIR-ATR analysis also successfully identified the unique spectral of each treatment method, while multivariate data analysis (MVDA) provided robust classification and discrimination of oils derived from different sources and processing techniques. Herein, this integrated approach demonstrates an efficient methodology for agarwood essential oil extraction and authentication, offering valuable insights for the fragrance, pharmaceutical, and cosmetic industries. By combining advanced spectroscopic techniques with statistical modelling, this study establishes a framework for quality assurance and traceability in the production of high-value natural products.

Keywords: Agarwood essential oils; Enzyme treatment; Microbial treatment; FTIR-ATR spectroscopy; Multivariate data analysis

Received: January 2025; Accepted: March 2025

Agarwood essential oil, such as agarwood oils derived from *Aquilaria* species of the *Thymelaeaceae* family, is obtained from 15 species around the world [1]. The highly valued fragrant oil has been used for centuries in various applications, including aromatherapy, medicine, and perfumery. Its unique fragrance and potential therapeutic properties has made it a highly sought-after commodity [2]. Meanwhile, the extraction and authentication of agarwood essential oils have long been challenging due to the intricate chemical composition and the limited yield of these precious essential oils. Regular extraction methods have been constrained by low efficiency, potential chemical degradation, and inconsistent quality control mechanisms. Moreover, the chemical complexity of agarwood essential oils represents a sophisticated molecular ecosystem characterized by diverse terpenoid, phenolic, and chromone-based compounds [3]. From a chemical perspective, the biosynthesis of these essential oils involves intricate biochemical pathways triggered by fungal elicitation, resulting in a rich spectrum of secondary metabolites with profound structural diversity. Furthermore, the increasing demand for essential oils has led to concerns about their authenticity and quality, as such adulteration, which is common practice in the essential oil industry that involves the addition of synthetic compounds or lower-quality oils to increase profit margins [4].

Enzymatic and microbial-assisted extraction methods offer significant advantages over the hydrodistillation method in extracting agarwood essential oils. The soaking method, which relies on passive diffusion, often results in low extraction efficiency, incomplete molecular release, and a lack of selectivity in targeting bioactive compounds. Additionally, prolonged soaking can lead to the loss of volatile components and unwanted chemical changes

due to extended exposure to water and ambient conditions. In contrast, enzymatic and microbial treatments enhance extraction efficiency by breaking down complex cell wall structures, facilitating a more effective release of essential oil components. These methods also allow for selective targeting of bioactive compounds through specific enzymatic or microbial actions, enriching the chemical profile while minimizing degradation. The enzymatic and microbial-assisted approaches enable controlled molecular modification, potentially improving the bioactivity, fragrance, and medicinal properties of the extracted oil. Operating under milder conditions, these methods help preserve heat-sensitive and volatile compounds, reducing the risk of chemical degradation. Additionally, they align with sustainable and eco-friendly extraction practices by minimizing the reliance on harsh chemical solvents. Thus, by strategically employing specific enzymatic catalysts and carefully selected microbial strains, researchers can potentially induce controlled chemical modifications, enhance extraction efficiency, and selectively target bioactive molecular constituents [5].

Conventional methods for the analysis of essential oils, such as gas chromatography-mass spectrometry (GC-MS), are highly accurate but time-consuming and require specialized equipment and expertise [6]. As a result, there is a growing need for rapid, reliable, and cost-effective techniques to authenticate and assess the quality of essential oils. Thus, the utilization of Fourier transform infrared-attenuated total reflectance (FTIR-ATR) spectroscopy represents a pivotal analytical breakthrough in molecular characterization. This spectroscopic technique provides unprecedented molecular fingerprinting capabilities, enabling comprehensive chemical profiling through vibrational spectroscopic analysis [7]. The molecular bond interactions captured by FTIR-ATR spectroscopy offer insights into the intricate chemical structural configurations of agarwood essential oils at a resolution previously unattainable through conventional analytical methodologies [8]. By analyzing the infrared spectrum of an essential oil, it is possible to identify specific functional groups and molecular structures, which can be used to assess its authenticity and quality. Multivariate statistical analyses further augment the chemical characterization process by enabling sophisticated pattern recognition, molecular classification, and chemometric interpretation of complex spectroscopic datasets. These advanced computational approaches transform raw spectroscopic data into meaningful chemical insights, facilitating detailed molecular structural elucidation and authentication [9].

Chemometric methods, such as principal component (PCA), discriminant (DA) and partial-least square-discriminant (PLS-DA) analyses, can be applied to FTIR-ATR spectra to extract meaningful information and classify samples based on their chemical profiles. PCA can identify patterns and trends in the data; DA distinguishes between two or more groups of samples by developing a predictive model using a set of known data, while PLS-DA can be used to build predictive models that can classify samples into different categories, such as genuine and adulterated essential oils [10]. Herein, the combination of FTIR spectroscopy and multivariate data analysis (MVDA) offers a powerful tool for the authentication and quality control of agarwood essential oils. By analyzing the spectral fingerprints of essential oils, it is possible to differentiate between genuine and adulterated samples, identify the botanical origin of the essential oils, and assess the quality [11].

Hitherto, this study aims to investigate the potential of FTIR-ATR spectroscopy coupled with chemometric analysis to authenticate agarwood essential oil by detecting unique spectral signatures resulting from different treatments. Furthermore, this research seeks to explore the potential of enzymatic and microbial-assisted extraction techniques as sustainable and efficient alternatives to traditional methods for the production of agarwood essential oil. By optimizing these techniques, it may be possible to increase the yield and quality of agarwood oil while reducing the environmental impact of the extraction process.

EXPERIMENTAL

Experimental Design

This study involved enzymatic and microbial-assisted treatments, followed by extraction and chemical analyses through functional and fingerprint regions of the wavenumber region of 4000 – 650 cm^{-1} using FTIR-ATR. The obtained FTIR-ATR spectra then underwent dataset pre-processing, transformation, and were subsequently analyzed using DA, PLS-DA and PCA analyses. **Figure 1** illustrates the experimental design for this research study.

Chemicals and Materials

Grounded agarwood chips from the species *Aquilaria subintegra* were obtained from a local agarwood farm located at Bukit Gambir, Muar, Johor, Malaysia. Meanwhile, the commercial samples of *Aquilaria subintegra* and *Aquilaria malaccensis* were obtained from Aromatic Bukit Rambai, a local agarwood oil producer located at Bukit Rambai, Melaka, Malaysia and a pilot-scale extraction of agarwood essential oil was obtained from Gaharu Research laboratory at ICA, UTM Pagoh. Diethyl ether, hydrochloric acid, and Viscozyme (MDL number: MFCD03101941) were purchased from Sigma Aldrich, USA, while *Lactobacillus acidophilus* NBRC 13951 was imported from Biological Resource Center, NITE, Japan. The Man, Rogosa and Sharpe (MRS) agar was purchased from Oxoid, UK. Glycerol was purchased from Merck, Germany. All chemicals were used as received without further purification.

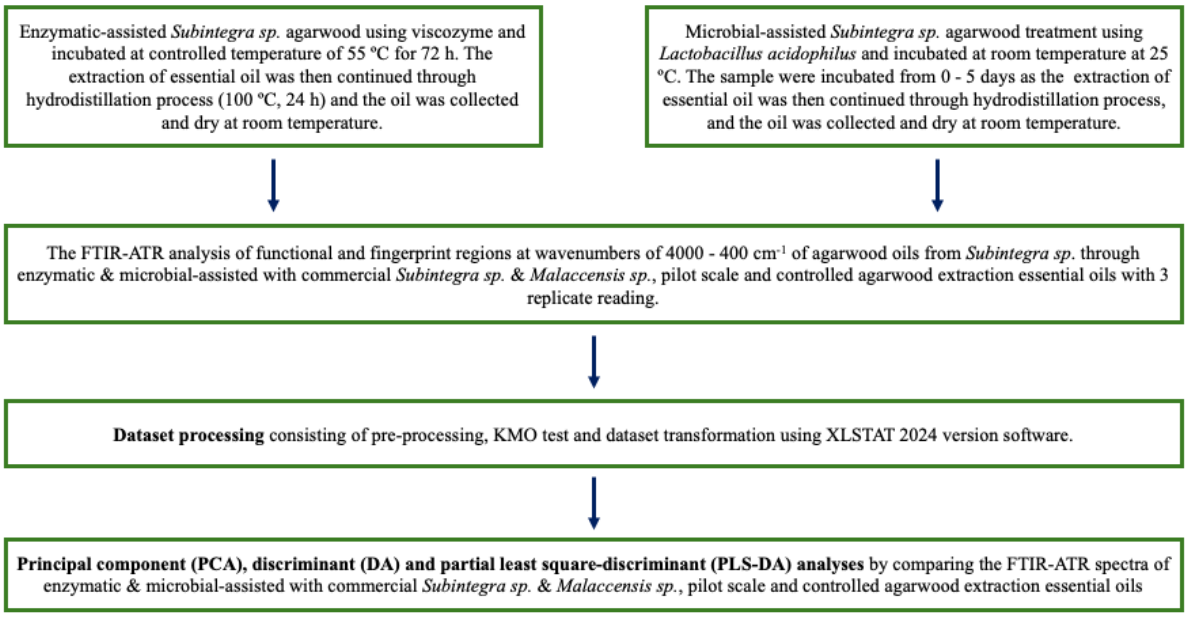

Figure 1. The design of experiment of enzymatic and microbial-assisted treatments, extraction, and authentication of agarwood essential oils using FTIR-ATR spectroscopy coupled with multivariate data analysis.

Preparation of Standard Hydrodistillation for Agarwood Oil Extraction

A Clevenger type apparatus, as shown in **Figure 2**, was used to extract the agarwood oil, following the procedure from Abdul Rahim *et al.* [12], with slight modifications. For the experiment, about 180 g of agarwood chips were transferred into a round bottom flask, followed by the addition of 1800 mL of distilled water. The hydrodistillation process was run for 24 h and the boiling temperature was maintained at 100ºC. A water chiller was used to cool down the condenser and was maintained at the temperature of 20ºC. After running for 24 h overnight, the oil formation was collected and the water layer was removed by double separation using diethyl ether and allowed to dry at room temperature. The weight of the collected oil was measured using an analytical balance.

Figure 2. The apparatus setup of standard hydrodistillation for agarwood essential oil.

Enzymatic-Assisted Treatment

The enzymatic-assisted extraction of agarwood oil was done according to the method of Rahim *et al.* [12], with modifications. The enzyme solution was prepared by adding 2.7 mL (1.5%, v/w) of Viscozyme into 1800 mL of distilled water and adjusting the pH to 5 using 0.1 M of HCl solution. A total of 180 g of agarwood chips was then added to the enzyme solution, and the mixture was incubated in an oven at 55°C for 72 h. After incubation, the oil was extracted using the same hydrodistillation setup described earlier. The resulting oil sample was labelled as E1.

Microbial-Assisted Treatment

The microbial-assisted method used to extract the agarwood essential oil was done according to the method by Monggoot *et al.* [14], with modifications. *L. acidophilus* NBRC 13951 was cultured on Man, Rogosa and Sharpe (MRS) agar at 25ºC for 48 h. 20% v/v glycerol of *L. acidophilus* was prepared and stored as a stock culture at -20ºC. For inoculum preparation, a single colony from the strain was sub-cultured in 50 mL of culture medium of MRS broth and incubated at 25ºC for 48 h. An aliquot of 10 mL of the cell suspension was then transferred into a conical flask containing 4000 mL of culture medium and incubated in an IN450Plus incubator (Memmert, Germany) at 25ºC. The inoculum was considered ready for use when it reached 1.0 corresponding to an approximate cell density of 10^8 CFU/mL by measuring the absorbance (OD) using the Cary 60 UV-VIS spectrophotometer (Agilent Technologies, USA) of each suspension at the 600 nm wavelength. Then, the microbial cells were precipitated from the medium by centrifugation (Kubota, Japan) at 8000 rpm at 10ºC for 20 min. The supernatant was collected, transferred into a sterile bottle and was kept at 4ºC until use. A total of 180 grams of *Aquilaria subintegra* agarwood wood chips was incubated with 1800 mL of supernatant of *L. acidophilus* at room temperature. Samples were incubated for 0 and 5 days to assess the effect of incubation time on the yield of agarwood oil. After incubation, the oil was extracted using the same hydrodistillation setup described earlier. The resulting agarwood essential oils were labelled as M1 and M51.

FTIR Analysis

The effects of the treatments on the chemical composition of the oil were analyzed using the Nicolet iS5 FTIR spectrophotometer (Thermo Scientific, USA) equipped with a diamond cell ATR accessory. The analysis was performed under a dry atmosphere at ambient temperature (25 ± 0.5°C) by placing a drop of the sample (commercial samples of *Aquilaria subintegra* (SC1) and *Aquilaria malaccensis* (MC1), pilot scale (PS1), C1, E1, M1, and M51) on the ATR diamond, ensuring full coverage. The spectral absorbance was recorded over the range of 4000 – 650 cm^{-1}, with a resolution of 4 cm^{-1} and 32 scans per measurement. A background spectrum was recorded before sample analysis, and each sample spectrum was baseline-corrected by subtracting the background spectrum. The results are presented in transmittance units. Three spectral replicates were obtained from three independent samples.

Data Pre-Processing

The spectra were compiled into comma-separated values (CVS) files and imported to the XLSTAT software (2024 version, France). The transmittance data were divided into specific wavenumber ranges: 4000 – 3501 cm^{-1}, 3500 – 3001 cm^{-1}, 3000 – 2501 cm^{-1}, 2500 – 2001 cm^{-1}, 2000 – 1501 cm^{-1}, 1500 – 1001 cm^{-1}, 1000 – 651 cm^{-1}, and 650 – 400 cm^{-1}. The key wavenumbers were identified and PCA was performed to determine the contribution of the aforementioned wavenumbers towards the extracted agarwood essential oils of the samples.

Kaiser-Meyer-Olkin (KMO) Test

Datasets were analyzed for dataset adequacy using the KMO test. An adequate dataset determines the ability to generate model to extract latent variables from the dataset. In this study, the KMO test was employed at a significant level (α) of 0.01. The calculated KMO was ranked as KMO < 0.5 = inadequate, 0.5 < KMO < 0.7 = mediocre, 0.7 < KMO < 0.8 = good, 0.8 < KMO < 0.9 = very good, and KMO > 0.9 = excellent to indicate the dataset adequacy, and only KMO > 0.5 was consider acceptable for PCA.

Dataset Transformation

To ensure that the datasets followed a normal distribution before PCA, the dataset normality was tested using the Shapiro-Wilk test at $\alpha = 0.05$. The datasets were transformed using standardized n-1, standardized (n), centre, standard deviation^{-1} (n-1), standard deviation (n), and Pareto transformation methods. The normal distribution of the transformed datasets was evaluated by the normality test of Shapiro-Wilk at $\alpha = 0.05$. The best transformation method and normality test were selected from the results.

Discriminant Analysis (DA)

DA established a discriminating model for all the enzymatic- and microbial-assisted treatments of the agarwood essential oils using the FTIR spectra database. A new column labelled as 'cluster' was added to the training and cross-validation datasets. The sample replicates of agarwood oils (SC1 – SC3) of *Aquilaria subintegra* and (MC1 – MC2) of *Aquilaria malaccensis* were assigned as "commercial agarwood essential oil", E1, E2 and E3 as "enzyme treatment agarwood essential oil", C1 – C3 as "control agarwood essential oil", PS1 – PS3 as "pilot scale

extraction agarwood essential oil", and M01 – M03 & M51 – M53 as "microbial treatment agarwood essential oil". The DA was executed of $\alpha = 0.01$ via the following Equation (1):

$$\boldsymbol{G_1 = h_0 + h_1 l_1 + h_2 l_2 + \cdots + h_i l_i} \quad (1)$$

to represent a linear model that combines the spectral features to discriminate between different classes. G_1 represents the discriminant score of the samples' FTIR spectra; h_0, is a constant, while l_1, l_2 and l_i are coefficients associated with each spectral feature of the wavenumber 4000 – 650 cm^{-1}, and h_1, h_2 and h_i are the spectral features based on the intensities at specific wavenumbers of all the samples. The *F*-statistics of $F_{observed}$ and $F_{critical}$ and the *p*-value of the Wilks' Lambda test were computed and the individual *F*-statistics and *p*-value of significant FTIR spectra were determined. Using the training and cross-validation datasets, correct classification of the clusters was examined, and the dissimilarities of commercial agarwood oils of *Aquilaria subintegra* and *Aquilaria malaccensis*, control, pilot scale extraction, and enzymatic and microbial-assisted extracted agarwood oils, respectively, were determined. The value of Fisher distance of the clusters and their *p*-value were also calculated to verify the cluster dissimilarity.

Partial-Least Squares – Discriminant Analysis (PLS-DA)

PLS-DA established a discriminating model for all the enzymatic- and microbial-assisted treatments of agarwood essential oils using the FTIR spectra database. A new column labelled as 'cluster' was added to the training and cross-validation datasets. Samples of agarwood oils (SC1 – SC3) of *Aquilaria subintegra* and (MC1 – MC2) of *Aquilaria malaccensis* were assigned as "commercial agarwood essential oil", E1, E2 and E3 as "enzyme treatment agarwood essential oil", C1 – C3 as "control agarwood essential oil", PS1 – PS3 as "pilot scale extraction agarwood essential oil", and M1 – M3 as "microbial treatment agarwood essential oil". The PLS-DA was carried out at $\alpha = 0.01$ on the training dataset to establish discriminating models for all the oil samples via Equation (2):

$$\boldsymbol{A(y_i, b_k) = c_0 + \sum_{f=1}^{d} h_i x_{if}} \quad (2)$$

The equation represents a linear model that projects the spectral data onto a latent variable space optimized for discriminating between classes. $A(y_i,b_k)$ represents the projection of the sample *i* onto a new latent variable space which is optimized to maximize the covariance between the spectral data of *X* and the class membership of *Y*. c_0 denotes the baseline value when all spectral feature values are zero. h_i is the weight corresponding to the latent variables, x_{if} is the transmittance value of the FTIR spectroscopy at specific wavenumbers, and d represents the total number of spectral wavenumbers used in the model.

The discriminant model represents the classification rule for assigning a sample to a class in a discriminant analysis model. In this context of FTIR spectroscopy analysis, the equation is used to classify a sample based on its spectral data and is represented into a class via Equation (3):

$$\boldsymbol{x = argmax_k A(y_i, b_k)} \quad (3)$$

The discriminant model returns the argument (*arg*) of *A* to the maximum class, *x* is the predicted class of label for sample *i*, and $A(y_i,b_k)$ denotes the discriminant score for sample *i* with the respect to class k. The goodness fit for the discriminant model was evaluated via R^2Y cumulated index, while the quality of the extracted oil contributors to the discriminant model was evaluated via the R^2X cumulated index. The ability of the discriminant model to classify the animal and plant clusters was measured via cross-validation of the PLS-DA and was represented as a Q^2 cumulated index. Cluster dissimilarity was also assessed via the Fisher distance and the distance *p*-values [13]. To validate the predictive ability of the discriminant model, the established model was validated and tested on cross-validation and testing datasets, respectively, and their percentage of correct classifications was evaluated. Based on the R^2Y, R^2X, Q^2, permutation test, Fisher distance, *p*-value, and percentage of correct classification in the training and cross-validation datasets, the classification ability of PLS-DA was obtained, and the best discriminant model was selected.

Principal Component Analysis (PCA)

The whole FTIR spectra was extracted of the transmittance values to obtain the dataset for PCA. The FTIR spectra at all the wavenumbers in the range of 4000 – 400 cm^{-1}. PCA was performed using the XLSTAT software, and the data were scaled using the Pareto scaling technique prior to PCA to maximize variation. The Pareto scaling helps by reducing the dominance of high-variance variables by ensuring that the principal components (PC) better represent the true underlying data structure rather than being skewed toward variables with large ranges. After Pareto scaling, the variables used for the PCA model were more normally distributed, shown by its Gaussian curve. The number of PCs was optimized to obtain optimum differentiation among samples. The differentiation result of samples was observed using a PCA score plot. Moreover, the PCA model was evaluated using its R^2 and Q^2 values to justify the good of fitness and predictivity of the PCA model, respectively.

RESULTS AND DISCUSSION

Extraction and Yield of Agarwood Essential Oils using Enzymatic and Microbial-Assisted Treatments

Table 1 shows the effects of pretreatment on the yield and characteristics of the agarwood oils. The control sample (C1) had the lowest oil yield at 0.069 g, while the enzymatic-assisted sample (E1) obtained 0.116 g (0.064%) of oil, which is an increase of 68%. Based on the observations shown in **Figure 3**, C1 oil has a thin consistency and a light-yellow color, whereas E1 oil has a much thicker consistency and a darker yellow color. These results indicate that enzymatic pretreatment effectively breaks down the wood fibers of agarwood, resulting in both a higher yield and a more concentrated oil. The darker color and increased yield of the E1 agarwood sample can be attributed to the comprehensive action of Viscozyme, which contains a mixture of carbohydrase enzymes. These enzymes systematically degrade complex plant cell wall components, including cellulose, hemicellulose, pectin, and lignin, thereby creating extraction pathways that release inner cell contents such as sesquiterpenes and sesquiterpenoids from the substrate (Yoswathana *et al.* [15]). This result is in agreement with the study reported by Rahim *et al.* [12], which reported the use of 3% cellulase enzyme in combination with the addition of 1% H_2SO_4. The addition of acid further improved enzyme accessibility to cellulose by affecting the ionization state of the enzyme, as well as the shape and charge of the substrate. This further supports the role of enzymatic treatment in improving extraction efficiency [14].

The microbial-assisted extractions showed higher yields compared to the control and the enzymatic treatment. The microbial supernatant, containing extracellular enzymes produced during the incubation stage, has been proven able to increase the yield of oil from agarwood chips [14]. Similar to enzymatic hydrolysis, microbial enzymes break down the wood fibers and loosen the wood structure, thus facilitating oil release during extraction. This process increases the porosity of the wood, allowing better penetration of the solvents or steam during the hydrodistillation step. The sample with no incubation (M1) produced 0.123 g (0.068%) of oil, while the extended incubation time of 120 hours (M51) resulted in the highest yield of 0.137 g (0.076%). Extended incubation time provides more time for the bacteria to produce and utilize the hydrolytic enzymes, resulting in a greater breakdown of the wood fiber and the release of oil bodies from the substrate, in accordance with Shaarani *et al.* [16]. In comparison with C1, the oil yield of M51 increased significantly by 98.5%. Both microbial-treated samples exhibited a pale yellow, medium-thick appearance but were similar to the C1 sample. *Lactobacillus acidophilus* was used in the microbial-assisted oil extraction method based on the study done by Monggoot *et al.*, and it was also selected due to its safety profile and widespread application in food and beverage production [14]. The results also showed that the microbial-assisted method is more efficient than the enzymatic hydrolysis in extracting the oil from the agarwood chips. Nevertheless, both enzymatic and microbial treatments significantly reduced the extraction time compared to conventional soaking methods, which typically require up to 7 days of soaking in water and has been demonstrated to have poor extraction efficiency.

Table 1. Oil yields from different treatment extraction approaches.

Sample Marking	Pretreatment	Incubation time (h)	Oil appearance (at RT)	Oil Yield (g)	Yield (%)
C1	-	0	Light yellow, thin	0.069^{a}	0.038
E1	Viscozyme	72	Bright yellow, thick	0.116^{b}	0.064
M1	*L. acidophilus*	0	Pale yellow, medium	0.123^{c}	0.068
M51	*L. acidophilus*	120	Pale yellow, medium	0.137^{d}	0.076

Remark: Values in the same column with different superscript letters are significantly different at $p<0.05$.

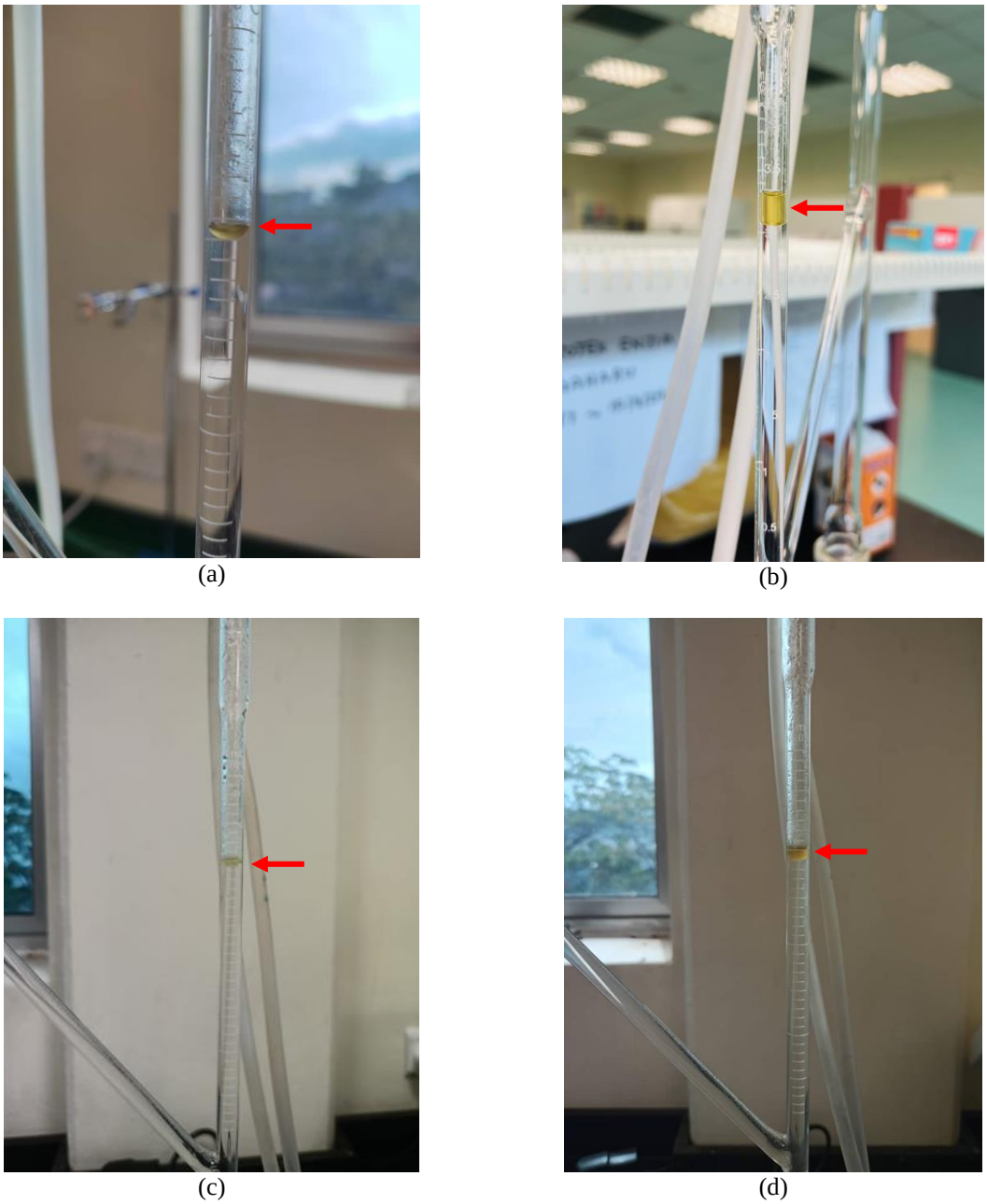

Figure 3. Different yields of agarwood essential oils observed as a pale-yellow viscous liquid with different volumes for different incubation times with Viscozyme and *L. acidophillus*: (a) control hydrodistillation; (b) enzyme incubated for 72 h; (c) incubation sample with microbial day 0; and (d) incubation sample with microbial day 5.

FTIR-ATR Spectral Analysis

FTIR-ATR spectroscopy was utilized to evaluate the effects of enzymatic treatment and microbial-assisted treatment on the chemical composition of agarwood essential oil. This approach has been reported as an effective method for evaluating the effects of different treatments in the extraction of oil from plant tissues [17,18]. The FTIR spectra of the oils of untreated agarwood (C1), enzymatically treated agarwood (E1), and microbial-assisted treatment at 0 and 5 days (M1 and M51) were analyzed. Additionally, the commercial essential oils derived from *Aquilaria malaccensis* (MC1) and *Aquilaria subintegra* (SC1), as well as oils obtained through pilot-scale (PS) extraction processes were also compared to assess the quality of the oils obtained, as shown in **Figure 4**.

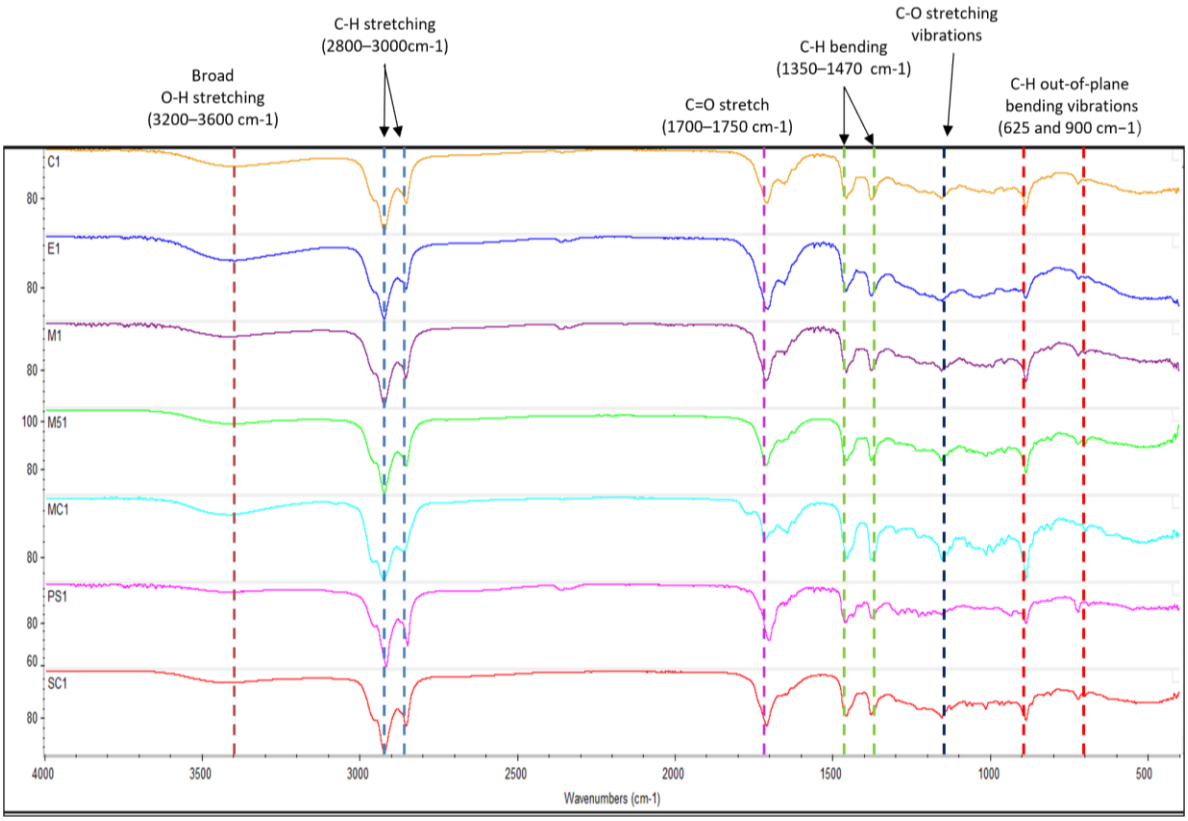

Figure 4. FTIR spectra of untreated agarwood essential oil (Control: C1), enzymatic treatment (E1), microbial treatment 0 and 5 days (M1, M51), ommercial agarwood oils of *Aquilaria malaccensis* (MC1) and *Aquilaria subintegra* (SC1), and pilot-scale extraction (PS1) in the wavenumber range of 4000 – 400 cm^{-1}.

Comparisons between commercial and pilot-scale oil products highlights the impact of extraction techniques on the final chemical profile. The spectrum of the untreated agarwood was nearly identical to those of the treated samples, indicating the important chemical compounds of agarwood are available. This suggests that the treatments can enhance extraction efficiency without causing significant changes or degradation of the chemical components. The chemical components of agarwood are essential because they determine its distinctive fragrance, therapeutic properties, and economic value. Agarwood oil is rich in sesquiterpenes, chromones, and other volatile organic compounds, which are primarily responsible for its characteristic aroma and are highly valued in the perfume and aromatherapy industries [19]. The major sesquiterpenes and monoterpenes in agarwood oil are α-gurjunene, α-guanine, β-himachalene, caryophyllene, and linalool [20,21]. **Figure 5** shows the major chemical structures of sesquiterpenes and monoterpenes which are found in agarwood oil.

Characteristic peaks associated with key functional groups were identified across all samples. The broad O–H stretching band observed in the range of 3600 – 3200 cm^{-1}, attributed to hydroxyl groups, is a significant marker for the presence of oxygenated compounds such as monoterpenes and sesquiterpenes, which are crucial for the aromatic properties of agarwood oil [22,23]. The C–H stretching vibrations in the range of 3000 – 2800 cm^{-1} indicate the presence of aliphatic hydrocarbons, while the C=O stretching band (1750 – 1700 cm^{-1}), indicative of carbonyl groups such as ketones, aldehydes, or esters, emphasized the retention of agarwood's resinous compounds [24]. The prominent aliphatic C=C stretching vibrations (1650 – 1600 cm^{-1}) confirmed the preservation of terpenes, which is integral to agarwood's chemical profile. Additionally, the C–O stretching vibrations (1300 – 1000 cm^{-1}), typically associated with esters and ethers, were present across all spectra, indicating the stability of oxygenated sesquiterpenes during treatments.

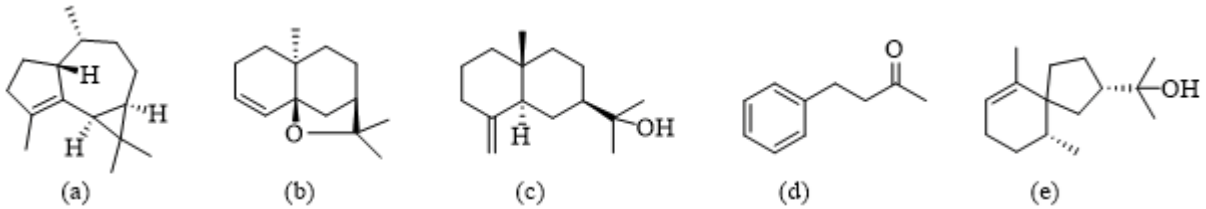

Figure 5. The major monoterpenes and sesquiterpenes in the essential oil of agarwood. (a) α-gurjunene, (b) β-agarofuran, (c) β-eudesmol, (d) 4-phenyl-2-butanone, and (e) agarospirol.

Specific vibrational modes related to monoterpenes, sesquiterpenes, and terpenes were also observed, reflecting the complexity of agarwood oil's composition. The C–H bending vibrations (1470 – 1350 cm^{-1}) and C=C stretching in conjugated terpenes (1640 – 1580 cm^{-1}) were particularly evident, indicating the presence of terpene-based compounds [24]. Monoterpenes and sesquiterpenes, which contribute significantly to the fragrance profile of agarwood oil, were detected through characteristic absorption bands such as C–H out-of-plane bending and cyclic C–O stretching, which were present in the range of 1150 – 1100 cm^{-1} and 900 – 880 cm^{-1}, respectively. These peaks were retained across untreated and treated samples, underscoring the effectiveness of the extraction processes in preserving agarwood's terpene-rich composition [25].

Comparisons between commercial oils (MS1, SC1) and the treated samples revealed distinct differences, likely stemming from additional processing methods such as distillation or blending in commercial production. In particular, the fingerprint region (900 – 600 cm^{-1}) exhibited variations, highlighting compositional differences between *Aquilaria malaccensis* and *Aquilaria subintegra* oils. Meanwhile, the pilot-scale extraction closely mirrored the spectra of untreated and treated agarwood, demonstrating that the scale-up process effectively maintained the chemical integrity of agarwood [26]. The FTIR-ATR analysis confirms that enzymatic and microbial-assisted treatments extract agarwood compounds without significantly altering their chemical structures. Retaining key functional groups (O–H, C–H, C=O, aliphatic C=C and C–O) ensures the chemical integrity of agarwood, validating its suitability for essential oil production. Minor spectral differences between treated samples and commercial oils highlight the impact of additional processing in commercial preparations [27].

Discriminant Analysis Model

The discriminant analysis (DA) model demonstrates a sophisticated statistical approach for classification across different wavenumber ranges, revealing nuanced insights into data discrimination capabilities. The analysis systematically evaluates model performance across multiple spectral regions, ranging from 650 – 400 cm^{-1} to 4000 – 3501 cm^{-1}, as shown in **Table 2**, with a consistent statistical significance (p-value<0.0001) and a significance level (α) of 0.01. Moreover, the DA model performance through the training, validation, and cross-validation datasets, whereby the analysis reveals significant findings, respectively [28].

At the lower wavenumber region of 650 – 400 cm^{-1}, the model demonstrated excellent discrimination in the training set with 100% correct classification. However, its performance notably declined in the validation and cross-validation sets, achieving only 33.33% correct classification for commercial, microbial, and pilot-scale samples. The model's Wilks' Lambda test yielded an $F_{observed}$ value of 847.814 (p<0.0001), indicating statistically significant discrimination ability.

Next, in the mid-range wavenumber region of 1500 – 1001 cm^{-1} exhibited remarkably robust performance, with the highest $F_{observed}$ value of 2132.813. This region showed exceptional classification accuracy, achieving 100% correct classification across most sample categories in both training and validation sets. The model also maintained strong performance in cross-validation, with classification accuracy ranging from 83.33% to 100% across different sample types. In the higher wavenumber regions of 3000 – 2501 cm^{-1}, the model maintained strong discriminatory power with an $F_{observed}$ value of 520.455. The training set maintained 100% accuracy, while validation and cross-validation sets showed consistent performance with 100% correct classification across most sample categories. This indicates the model's robust ability to discriminate between different sample types in this spectral region.

Lastly, the highest wavenumber region of 4000 – 3501 cm^{-1} showed slightly reduced but still significant discriminatory power, with an $F_{observed}$ value of 21.571. While maintaining perfect classification in the training set, the validation accuracy varied, with commercial samples showing 50% accuracy while other categories maintained 100% accuracy. Moreover, all analyses were conducted at α = 0.01 significance level, with p-values consistently below 0.0001, indicating strong statistical significance across all wavenumber regions. The $F_{critical}$ values remained consistent across most regions, ranging from 2.608 to 6.857, providing a reliable baseline for assessing model performance. This comprehensive analysis suggests that the mid-range wavenumber region of 1500 – 1001 cm^{-1} provides the most reliable discriminatory power for sample classification while

maintaining robust performance across different validation methods. The model's performance generally decreased at extreme wavenumber regions, particularly in the lower range, suggesting these regions may be less suitable for reliable sample discrimination.

Table 2. Classification matrix of training, validation and cross-validation datasets of discriminant analysis of commercial, control, enzymatic, microbial, and pilot scale agarwood essential oils.

Discriminating model at wavenumber (cm^{-1})	Discriminating model quality Wilks' Lambda Test				Dataset	Correct classification %
	$F_{observed}$	$F_{critical}$	*p*-value	α		
650 - 400	847.814	6.857	<0.0001	0.01	Training	
					Commercial	100
					Control	100
					Enzyme	100
					Microb	100
					Pilot Scale	100
					Validation	
					Commercial	0
					Control	0
					Enzyme	0
					Microb	0
					Pilot Scale	0
					Cross-Validation	
					Commercial	33.33
					Control	0
					Enzyme	0
					Microb	33.33
					Pilot Scale	33.33
1000 – 651	821.445	6.857	<0.0001	0.01	Training	
					Commercial	100
					Control	100
					Enzyme	100
					Microb	100
					Pilot Scale	100
					Validation	
					Commercial	100
					Control	0
					Enzyme	0
					Microb	0
					Pilot Scale	0
					Cross-Validation	
					Commercial	40
					Control	0
					Enzyme	33.33
					Microb	100
					Pilot Scale	66.67
1500 – 1001	2132.813	4.110	<0.0001	0.01	Training	
					Commercial	100
					Control	100
					Enzyme	100
					Microb	100
					Pilot Scale	100

					Validation	
					Commercial	0
					Control	0
					Enzyme	0
					Microb	100
					Pilot Scale	0
					Cross-Validation	
					Commercial	83.33
					Control	100
					Enzyme	100
					Microb	100
					Pilot Scale	100
					Training	
					Commercial	100
					Control	100
					Enzyme	100
					Microb	100
					Pilot Scale	100
					Validation	
					Commercial	0
					Control	0
2000 – 1501	903.085	6.857	<0.0001	0.01	Enzyme	0
					Microb	100
					Pilot Scale	0
					Cross-Validation	
					Commercial	83.33
					Control	100
					Enzyme	100
					Microb	100
					Pilot Scale	100
					Training	
					Commercial	100
					Control	100
					Enzyme	100
					Microb	100
					Pilot Scale	100
					Validation	
					Commercial	0
					Control	0
2500 – 2001	111.534	6.857	<0.0001	0.01	Enzyme	100
					Microb	0
					Pilot Scale	0
					Cross-Validation	
					Commercial	100
					Control	100
					Enzyme	100
					Microb	50
					Pilot Scale	100
					Training	
					Commercial	100
3000 – 2501	520.455	2.838	<0.0001	0.01	Control	100
					Enzyme	100
					Microb	100

					Pilot Scale	100
					Validation	
					Commercial	0
					Control	0
					Enzyme	100
					Microb	0
					Pilot Scale	0
					Cross-Validation	
					Commercial	100
					Control	100
					Enzyme	100
					Microb	100
					Pilot Scale	100
					Training	
					Commercial	100
					Control	100
					Enzyme	100
					Microb	100
					Pilot Scale	100
					Validation	
					Commercial	0
					Control	0
3500 – 3001	36.754	2.608	<0.0001	0.01	Enzyme	0
					Microb	100
					Pilot Scale	0
					Cross-Validation	
					Commercial	66.67
					Control	100
					Enzyme	100
					Microb	100
					Pilot Scale	100
					Training	
					Commercial	100
					Control	100
					Enzyme	100
					Microb	100
					Pilot Scale	100
					Validation	
					Commercial	0
					Control	0
4000 – 3501	21.571	2.838	<0.0001	0.01	Enzyme	0
					Microb	100
					Pilot Scale	0
					Cross-Validation	
					Commercial	50
					Control	100
					Enzyme	100
					Microb	100
					Pilot Scale	100

Partial Least Squares - Discriminant Analysis (PLS-DA) Model

The study employed PLS-DA across eight distinct wavenumber regions spanning from 400 to 4000 cm^{-1}, with each region evaluated through multiple quality parameters that collectively provide insights into the model's discriminative capabilities, as shown in **Table 3**, respectively. The analysis framework incorporated three critical evaluation metrics: R^2Y representing the model's fit to dependent variables, R^2X indicating the model's fit to independent variables, and Q^2 quantifying the model's predictive ability. Notably, all analyzed regions demonstrated statistical significance with p-values<0.01, establishing a fundamental basis for model reliability across the spectral range [29].

The most compelling performance was observed in the mid-infrared regions of 2000 – 1501 cm^{-1} and 2500 – 2001 cm^{-1}, which exhibited superior predictive capabilities with Q^2 values of 0.215 and 0.253, respectively. These regions demonstrated exceptional model fits with remarkably high R^2X values (0.939 and 0.998, respectively), though moderately strong R^2Y values (0.345 and 0.341, respectively). The achievement of 100% classification accuracy in the training dataset for these regions underscores their robust discriminative power, suggesting these aforementioned spectral regions contain highly informative molecular fingerprints that effectively differentiate between sample classes.

In contrast, the spectral regions below 1500 cm^{-1} exhibited comparatively weaker performance metrics. Despite maintaining high R^2X values exceeding 0.866, these regions were characterized by notably lower R^2Y values (approximately 0.17) and Q^2 values ranging from 0.074 to 0.118. This pattern, combined with highly variable classification accuracies (16.67% to 100%), suggests potential model instability and overfitting in these lower wavenumber regions. The discrepancy between training and validation set performances further emphasizes this limitation, with validation accuracies consistently lower across all spectral regions, particularly evident in commercial and control sample classifications.

A crucial observation lies in the model's generalization capabilities, as evidenced by the validation dataset results. The systematic decrease in classification accuracy from training to validation sets across all spectral regions indicates inherent challenges in model transferability. This phenomenon is particularly pronounced in the classification of commercial and control samples, where accuracy fluctuations across different spectral regions suggest varying levels of spectral feature relevance and stability. The performance disparity between training and validation sets emphasizes the importance of careful model optimization and validation strategies in practical applications.

The comprehensive analysis reveals that while PLS-DA demonstrates considerable potential as a discriminative tool, its effectiveness is highly dependent on the selected spectral region. The superior performance in the mid-range wavenumbers (2500 – 1501 cm^{-1}) suggests these regions contain the most reliable and informative spectral features for classification purposes. This finding has significant implications for future applications, indicating that focused analysis within these optimal spectral regions might yield more robust and reliable classification results. The observed patterns also underscore the importance of thorough validation procedures and careful consideration of spectral region selection in developing practical PLS-DA applications for sample classification and discrimination tasks.

Table 3. Classification matrix of training and validation datasets of partial least squares - discriminant analysis of commercial, control, enzymatic, microbial and pilot scale agarwood essential oils.

Discriminating model at wavenumber (cm^{-1})	Discriminating model quality R^2Y, R^2X and Q^2 cumulated indices and permutation test				Dataset	Correct classification %
	R^2Y	R^2X	Q^2	p-value		
650 - 400	0.177	0.984	0.118	p<0.01	Training dataset	
					Commercial	16.67
					Control	0
					Enzyme	100
					Microb	50
					Pilot Scale	0
					Validation dataset	
					Commercial	0
					Control	0
					Enzyme	0
					Microb	0
					Pilot Scale	0

1000 - 651	0.168	0.914	0.105	$p<0.01$	Training dataset	
					Commercial	0
					Control	0
					Enzyme	100
					Microb	83.33
					Pilot Scale	0
					Validation dataset	
					Commercial	0
					Control	0
					Enzyme	0
					Microb	0
					Pilot Scale	0
1500 - 1001	0.168	0.866	0.109	$p<0.01$	Training dataset	
					Commercial	20
					Control	0
					Enzyme	100
					Microb	100
					Pilot Scale	0
					Validation dataset	
					Commercial	0
					Control	0
					Enzyme	0
					Microb	0
					Pilot Scale	0
2000 - 1501	0.345	0.939	0.215	$p<0.01$	Training dataset	
					Commercial	100
					Control	0
					Enzyme	100
					Microb	60
					Pilot Scale	0
					Validation dataset	
					Commercial	0
					Control	0
					Enzyme	0
					Microb	0
					Pilot Scale	0
2500 - 2001	0.341	0.998	0.253	$p<0.01$	Training dataset	
					Commercial	100
					Control	0
					Enzyme	0
					Microb	50
					Pilot Scale	100
					Validation dataset	
					Commercial	100
					Control	0
					Enzyme	0
					Microb	0
					Pilot Scale	0
3000 - 2501	0.135	0.884	0.074	$p<0.01$	Training dataset	
					Commercial	50
					Control	0
					Enzyme	0
					Microb	60
					Pilot Scale	66.67

					Validation dataset	
					Commercial	0
					Control	0
					Enzyme	0
					Microb	0
					Pilot Scale	0
3500 - 3001	0.131	0.943	0.079	p<0.01	Training dataset	
					Commercial	20
					Control	0
					Enzyme	100
					Microb	50
					Pilot Scale	0
					Validation dataset	
					Commercial	0
					Control	0
					Enzyme	0
					Microb	0
					Pilot Scale	0
4000 - 3501	0.125	0.984	0.092	p<0.01	Training dataset	
					Commercial	100
					Control	0
					Enzyme	0
					Microb	60
					Pilot Scale	0
					Validation dataset	
					Commercial	0
					Control	0
					Enzyme	0
					Microb	0
					Pilot Scale	0

Principal Component Analysis (PCA)

PCA was used in this study to reduce all the chemical structures comprising of functional and fingerprint regions from the FTIR-ATR spectroscopy wavenumber range of 4000 – 400 cm^{-1}, as this technique can be considered as preferable and approachable to understand more deeply by combining chemical and statistical analyses [30]. The PCA results presented in **Figure 6** provide a comprehensive overview of the variance structure and clustering behavior among the analyzed samples. Each subplot, Figures 6(a) – (h), represents observations distributed along the first two principal components (F1 and F2), which cumulatively account for a substantial proportion of the total variance, ranging from 91.55 – 99.38% (plots a – d) to over 95.80 – 99.80% (plots e – h) from the wavenumber range of 650 – 400 cm^{-1}, 1000 – 651 cm^{-1}, 1500 – 1001 cm^{-1}, 2000 – 1501 cm^{-1}, 2500 – 2001 cm^{-1}, 3000 – 2501 cm^{-1}, 3500 – 3001 cm^{-1}, and 4000 – 3501 cm^{-1}, respectively. This highly explained variance indicates that the dimensionality reduction is effective, and the two components capture the majority of meaningful patterns in the datasets.

In the meanwhile, the KMO measure of sampling adequacy is a statistic used to assess the suitability of data for factor analysis, evaluating the proportion of variance among variables that might be a common variance. The closer the KMO value is to 1, the more appropriate the data is for factor analysis, with thresholds generally interpreted as follows: values above 0.8 are considered excellent, between 0.7–0.8 as good, 0.6–0.7 as moderate, and below 0.6 as inadequate. Based on the data in **Table 4**, the KMO values for different wavenumber ranges are all well above 0.8, indicating an excellent level of sampling adequacy across the spectrum. The specific KMO values range from 0.803 to 0.910, with the highest adequacy observed in the 4000–3501 cm^{-1} (0.910) and 2500–2001 cm^{-1} (0.905) regions. This reflects a high proportion of shared variance, suggesting that the dataset is robust and well-suited for subsequent multivariate statistical analyses, such as factor analysis or the PCA [31]. These results underscore the reliability of the sampling and the effectiveness of the spectral regions in capturing the underlying data structure.

Table 4. Sampling adequacy test through Kaiser-Meyer-Olkin (KMO) test.

KMO measure of sampling adequacy:
Wavenumber (650 – 400 cm^{-1}) = 0.874
Wavenumber (1000 – 650 cm^{-1}) = 0.866
Wavenumber (1500 – 1001 cm^{-1}) = 0.803
Wavenumber (2000 – 1501 cm^{-1}) = 0.860
Wavenumber (2500 – 2001 cm^{-1}) = 0.905
Wavenumber (3000 – 2501 cm^{-1}) = 0.852
Wavenumber (3500 – 3001 cm^{-1}) = 0.902
Wavenumber (4000 – 3501 cm^{-1}) = 0.910

As distinct clustering patterns are observed across the PCA plots, this suggests inherent groupings within the datasets. For instance, green represents the commercial agarwood oils, orange represents the pilot-scale extraction oils, purple represents the enzymatic-assisted extraction oils, and black represents the microbial-assisted extraction oils, which delineate clusters of samples with shared characteristics, potentially corresponding to similar chemical compositions or experimental treatments. These groupings are consistently observed across multiple subplots, underscoring the robustness of the clustering patterns and their potential relevance in explaining the dataset's underlying variability. The distinct separation of certain clusters, such as the black and green clusters, could indicate significant differences between groups, possibly due to differences in their physical, chemical, or biological attributes.

Moreover, **Figure 6** depicts the PCA clustering results for agarwood essential oils derived from commercial, pilot-scale, and control while including different processing treatments as such enzymatic and microbial, respectively. The clustering was performed based on FTIR-ATR spectra recorded within the wavenumber range of 4000 – 400 cm^{-1}. For detailed spectral analysis, the data were categorized into eight distinct subregions: (a) 650 – 400 cm^{-1}; (b) 1000 – 650 cm^{-1}; (c) 1500 – 1001 cm^{-1}; (d) 2000 – 1501 cm^{-1}; (e) 2500 – 2001 cm^{-1}; (f) 3000 – 2501 cm^{-1}; (g) 3500 – 3001 cm^{-1}; and (h) 4000 – 3501 cm^{-1}. Among these spectral subregions, the PCA plots corresponding to the wavenumber ranges of (a) 650 – 400 cm^{-1}, (c) 1500 – 1001 cm^{-1}, and (f) 3000 – 2501 cm^{-1} exhibited the most distinct and well-defined clustering, effectively differentiating all the commercial, control, enzymatic, microbial, and pilot-scale agarwood essential oil samples. This pronounced separation suggests that these specific spectral regions capture key chemical variations among the samples, likely attributable to differences in chemical composition resulting from the distinct extraction and processing techniques employed [32,33]. These findings demonstrate the effectiveness of FTIR-ATR spectroscopy combined with PCA as a reliable technique for characterizing and distinguishing agarwood essential oils based on their chemical profiles. Noteworthy, the PCA analysis effectively reduces the datasets' complexity while maintaining the essential variability. The clustering behavior and separation observed provide valuable insights into the relationships among the samples, highlighting potential distinctions in their characteristics. Further interpretation and integration of metadata are essential to elucidate the specific factors driving these groupings and to draw meaningful conclusions. These findings could have significant implications for the studied system, such as identifying critical variables influencing sample differentiation or validating classification models in future studies.

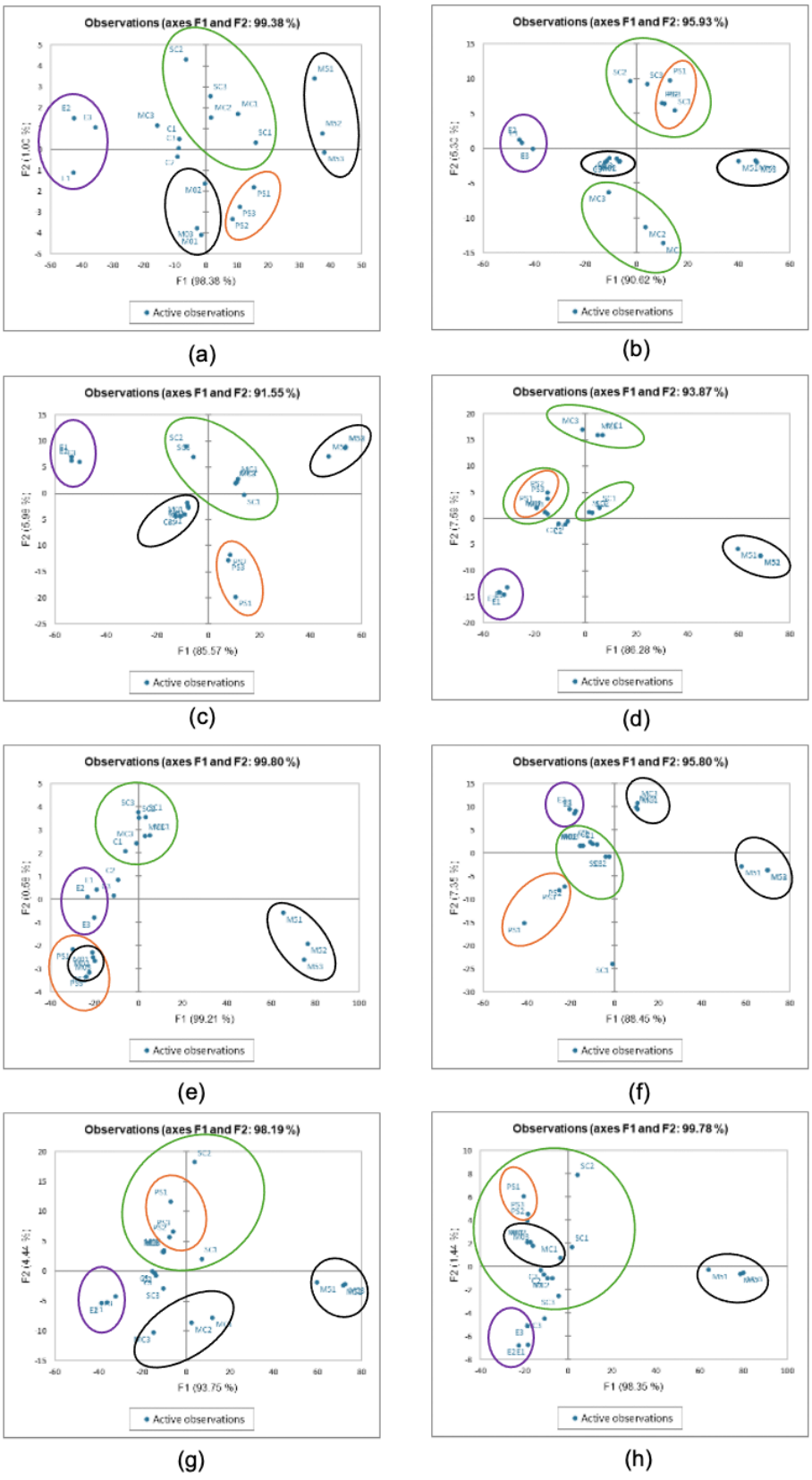

Figure 6. Combined PCA score plots of all FTIR-ATR dataset transformation of the wavenumber region of 4000 – 400 cm^{-1} of commercial, control, enzymatic, microbial, and pilot-scale agarwood essential oils. FTIR-ATR wavenumber regions of (a) 650 – 400 cm^{-1}; (b) 1000 – 650 cm^{-1}; (c) 1500 – 1001 cm^{-1}; (d) 2000 – 1501 cm^{-1}; (e) 2500 – 2001 cm^{-1}; (f) 3000 – 2501 cm^{-1}; (g) 3500 – 3001 cm^{-1}; and (h) 4000 – 3501 cm^{-1}.

CONCLUSION

FTIR-ATR spectroscopy coupled with MVDA techniques, such as DA, PLS-DA and PCA, has been shown to be a useful, powerful, and sophisticated tool for quantifying and discriminating agarwood essential oils obtained different treatment methodologies. Moreover, comparative analyses of enzymatic and microbial-assisted treatments against controlled, commercial, and pilot-scale extraction highlight the potential of microbial pre-treatment as the optimal approach for extraction and producing high-quality agarwood essential oil. This is supported by PCA of the FTIR spectral data, which reveals a strong correlation between microbial pre-treatment and commercial methodology, particularly within the wavenumber ranges of 650 – 400 cm^{-1}, 1500 – 1001 cm^{-1}, and 3000 – 2501 cm^{-1}, respectively. These findings suggest that microbial-assisted pre-treatment is a promising method for future application of agarwood essential oil extraction in the industry.

CONFLICT OF INTEREST

All authors declare that they have no competing interests that could have appeared to influence the work reported in this research paper.

ACKNOWLEDGEMENT

The authors recognize Innovation Centre in Agritechnology for Advanced Bioprocessing (ICA), Universiti Teknologi Malaysia (Pagoh Campus) for supporting and providing the facilities for the present work, as well as the funding from Universiti Teknologi Malaysia (UTM) under the grants QuickWin Research [Grant No.: R.J130000.7754.4J628] and UTM Contract Research DTD [Grant No.: R.J130000. 7654.4C754].

REFERENCES

1. Shivanand, P., Arbie, N. F., Krishnamoorthy, S. & Ahmad, N. (2022) Agarwood—the fragrant molecules of a wounded tree. *Molecules*, **27(11)**, 3386.

2. Tock, M. L. A., Kamatou, G. P. P., Combrinck, S., Sandasi, M. & Viljoen, A. M. (2020) A Chemometric Assessment of Essential Oil Variation of Three *Salvia* Species Indigenous to South Africa. *Phytochemistry*, **172**, 112249.

3. Ahmad, I., Fikri, J. A. N., Arifianti, A. E., Abdullah, S. & Munim, A. (2022) The Combination of ATR-FTIR and Chemometrics for Rapid Analysis of Essential Oil from *Myrtaceae* Plants–A review. *Journal of Applied Pharmaceutical Science*, **12(6)**, 30–42.

4. Huzir, S. M. H. M., Tajuddin, S. N., Yusoff, Z. M., Ismail, N., Abd Almisreb, A. & Taib, M. N. (2024) Agarwood Oil Quality Identification using Artificial Neural Network Modelling for Five Grades. *International Journal of Electrical and Computer Engineering (IJECE)*, **14(2)**, 2254–2261.

5. Rodrigues, D., Sousa, S., Silva, A., Amorim, M., Pereira, L., Rocha-Santos, T. A., Gomes, A. M. P., Duarte, A. C. & Freitas, A. C. (2015) Impact of Enzyme-and Ultrasound-Assisted Extraction Methods on Biological Properties of Red, Brown, and Green Seaweeds from the Central West Coast of Portugal. *Journal of Agricultural and Food Chemistry*, **63(12)**, 3177–3188.

6. Wang, M. R., Li, W., Luo, S., Zhao, X., Ma, C. H. & Liu, S. X. (2018) GC-MS Study of the Chemical Components of Different *Aquilaria sinensis* (*Lour.*) Gilgorgans and Agarwood from Different Asian Countries. *Molecules*, **23(9)**, 2168.

7. Khalil, A. S., Rahim, A. A., Taha, K. K. & Abdallah, K. B. (2013) Characterization of Methanolic Extracts of Agarwood Leaves. *Journal of Applied and Industrial Sciences*, **1(3)**, 78–88.

8. Zainuddin, N. A. S., Ku Hamid, K. H., Musa, M. & Rodhi, M. N. M. (2014) Effect of Hydrochloric Acid (HCl) Treatment on FTIR Profile of Agarwood Waste from Hydrodistillation Process. *Applied Mechanics and Materials*, **575**, 165–169.

9. Chen, Y., Yan, T., Zhang, Y., Wang, Q. & Li, G. (2020) Characterization of the Incense Ingredients of Cultivated Grafting Kynam by TG-FTIR and HS-GC-MS. *Fitoterapia*, **142**, 104493.

10. Sen, S., Dehingia, M., Talukdar, N. C. & Khan, M. (2017) Chemometric Analysis Reveals Links in the Formation of Fragrant Bio-Molecules during Agarwood (*Aquilaria malaccensis*) and Fungal Interactions. *Scientific reports*, **7(1)**, 44406.

11. Li, J., Yu, L., Liang, Y., Lan, B., Chen, Y., Wang, Q. & Wu, Z. (2024) Chemical Analysis of Different Parts from Agarwood Columns by Artificially Agarwood-Inducing Method based on GC–MS and UPLC-TOF-MS. *Fitoterapia*, **178**, 106156.

12. Rahim, A. F. A., Kadri, A. & Harun, N. M. (2019) The Effect of Enzymatic Pre-Treatment in Agarwood Oil Extraction. *International Journal*

of Advanced Science Engineering Information Technology, **9(4)**, 1317–1323.

13. Lasalvia, M., Capozzi, V. & Perna, G. (2022) A Comparison of PCA-LDA and PLS-DA Techniques for Classification of Vibrational Spectra. *Applied Sciences*, **12(11)**, 5345.

14. Monggoot, S., Kulsing, C., Wong, Y. F. & Pripdeevech, P. (2018) Incubation of *Aquilaria subintegra* with Microbial Culture Supernatants Enhances Production of Volatile Compounds and Improves Quality of Agarwood Oil. *Indian Journal of Microbiology*, **58**, 201–207.

15. Yoswathana, N., Eshiaghi, M. N. & Jaturapornpanich, K. (2012) Enhancement of Essential Oil from Agarwood by Subcritical Water Extraction and Pretreatments on Hydrodistillation. *International Journal of Chemical and Molecular Engineering*, **6(5)**, 459–465.

16. Shaarani, S. M., Min, L. Y., Man, R. C., Mudalip, S. K. A., Sulaiman, S. Z. & Arshad, Z. I. M. (2021) Effects of Enzyme Loading, Incubation Time and Incubation Temperature on Sawdust Hydrolysis by Locally Produced Bacterial Xylanase. *Journal of Chemical Engineering and Industrial Biotechnology*, ***7*(1)**, 14–22.

17. Ikhsan, A. N., Rohman, A., Putri, A. R., Syifa, F., Mustafidah, M. & Martien, R. (2021) Application of FTIR Spectroscopy and Chemometrics for the Prediction of Radical Scavenging Activities of Fish Oils. *Indonesian Journal of Pharmacy*, 166–174.

18. Mekonnen, K. D. (2023) Fourier Transform Infrared Spectroscopy as a Tool for Identifying the Unique Characteristic Bands of Lipid in Oilseed Components: Confirmed via Ethiopian Indigenous Desert Date Fruit. *Heliyon*, **9(4)**, e14699.

19. Yan, T., Yang, S., Chen, Y., Wang, Q. & Li, G. (2019) Chemical Profiles of Cultivated Agarwood Induced by Different Techniques. *Molecules*, **24(10)**, 1990.

20. Radzi, N. C., Harip, M. K. Z., Musa, M., Zaki, N. A. M., Alwi, H., Rodhi, M. N. M. & Hamid, K. H. K. (2018) Analysis of Sesquiterpenes in Agarwood Essential Oil from Hydrodistillation Process. *Malaysian Journal of Analytical Sciences*, **22(2)**, 353–357.

21. Shaian, H. E., Aizal, C. M. & Tajuddin, S. N. (2021) Chemical Composition of Agarwood Essential Oil (*Aquilaria malaccensis*) Upon Exposure Towards Heat Condition. *Malaysian Journal of Chemistry*, **23(2)**, 199–204.

22. Al-Farsi, R., Al-Yahyai, S. & Khan, S. (2020) Comparative Analysis of Essential Oils Extracted through Microbial Fermentation and Conventional Methods. *Journal of Natural Products*, **83(7)**, 2023–2030

23. Gao, M., Han, X., Sun, Y., Chen, H., Yang, Y., Liu, Y. Meng, H., Gao Z., Xu, Y., Zhang, Z. & Han, J. (2019). Overview of Sesquiterpenes and Chromones of Agarwood Originating from Four Main Species of the Genus *Aquilaria*. *RSC Advances*, **9(8)**, 4113–4130.

24. Wang, S., Yu, Z., Wang, C., Wu, C., Guo, P. & Wei, J. (2018) Chemical Constituents and Pharmacological Activity of Agarwood and *Aquilaria* Plants. *Molecules*, **23(2)**, 342.

25. Naef, R. (2011) The Volatile and Semi-Volatile Constituents of Agarwood, the Infected Heartwood of *Aquilaria* Species: A Review. *Flavour and Fragrance Journal*, **26(2)**, 73–87.

26. Zhang, N., Xue, S., Song, J., Zhou, X., Zhou, D., Liu, X., Hong, Z. & Xu, D. (2021) Effects of Various Artificial Agarwood-Induction Techniques on the Metabolome of *Aquilaria sinensis*. *BMC Plant Biology*, **21**, 1–13.

27. Li, W., Chen, H. Q., Wang, H., Mei, W. L. & Dai, H. F. (2021) Natural Products in Agarwood and *Aquilaria* Plants: Chemistry, Biological Activities and Biosynthesis. *Natural Product Reports*, **38(3)**, 528–565.

28. Adi, D. S., Hwang, S. W., Pramasari, D. A., Amin, Y., Widyaningrum, B. A., Darmawan, T., Septiana, E., Dwianto, W. & Sugiyama, J. (2020) Spectral Observation of Agarwood by Infrared Spectroscopy: The Differences of Infected and Normal *Aquilaria microcarpa*. *Biodiversitas Journal of Biological Diversity*, **21(7)**, 2893–2899.

29. Grosskopf, E. K., Simmonds, M. S. & Wallis, C. J. (2023) Combining Near-Infrared (NIR) Analysis and Modelling as a Fast and Reliable Method to Determine the Authenticity of Agarwood (*Aquilaria spp.*). *Analytica*, **4(2)**, 231–238.

30. Nazri, M. Z., Abd Rashid, S. N. A., Ab Malik, S., A. Karim, H. A., Abdullah Sani, M. S. & Abang Zaidel, D. N. (2024) The FTIR-ATR Spectroscopy and Multivariate Data Analysis (MVDA) for *Halal* Authentication of Animal Fatty Acids. *Malaysian Journal of Chemistry*, **26(6)**, 184–193.

31. Sani, M. S. A., Ismail, A. M., Azid, A., Samsudin, M. S. & Yuswan, M. H. (2024) Incorporation of Partial Least Squares-Discriminant Analysis with Ultra-High-Performance Liquid

Chromatography Diode-Array Detector for Authentication of Skin Gelatine Sources. *Halalsphere*, **4(1)**, 1–13.

32. Azah, M. N., Ismail, N., Mailina, J., Taib, M. N., Rahiman, M. H. F. & Hafizi, Z. M. (2014) Chemometric Study of Selected Agarwood Oils by Gas Chromatography—Mass Spectrometry. *Journal of Tropical Forest Science*, **26(3)**, 382–388.

33. Putra, W. P. B., Said, S. & Arifin, J. (2020) Principal Component Analysis (PCA) of Body Measurements and Body Indices in the Pasundan Cows. *Black Sea Journal of Agriculture*, **3(1)**, 49–55.